Development of an optical multi-purpose sensor using filtered scattered light

Guido Stockhausen[1,*], Andreas Enns[1], Ulrich Doll[1], Manfred Beversdorff[1], Christian Willert[1]

1: Institute of Propulsion Technology, German Aerospace Center (DLR), 51170 Koeln, Germany
* correspondent author: guido.stockhausen@dlr.de

Abstract We present the development of an optical sensor head which consists of a confocal backscatter arrangement of lenses and light guiding fibers. Using a molecular absorption cell which contains iodine vapor different scatter techniques are employed to obtain multiple flow field parameters in different media like gas and liquids. For velocity measurements filtered Mie scattering is used and validation experiments with a free jet yield an absolute error of 2m/s. In gaseous flows the sensor applies filtered Rayleigh scattering to determine temperature values with an accuracy of +/-3K and pressure values which show a systematic deviation of -2% from reference measurements. Finally filtered Brillouin scattering is introduced for measuring the temperature in liquids like tap water. This technique agrees within 1K when compared to a conventional thermo element measurement.

1. Introduction

Technical breakthroughs and rapid progress in laser science and related optical components like fibers, filters and detectors have enabled the development of various optical sensors. Laser Doppler anemometers (LDA), Laser vibrometers, distributed temperature sensing systems (DTS) or fluorescence systems are state-of-the-art measurement technologies commercially available as probes and therefore suitable to determine physical properties even in environments with limited access. Another advantage of these optical sensors is the non-intrusive use in the sense that they don't disturb the flow environment through the presence of a probe body in contrast to conventional systems like pitot tubes or hot-wire anemometers. While the application of LDA and DTS sensors are widely used a compact and reliable optical sensor capable of measuring the temperature or pressure inside a given flow volume is still work in progress.
One possible solution is the extraction of temperature and/or pressure information from the spectral profiles of Rayleigh and Brillouin scattered light from gases and liquids respectively as demonstrated by LIDAR systems [5, 6]. To eliminate the disturbing influences from surfaces, dust or suspended particles a molecular filter can be applied in form of an iodine absorption cell in combination with these spectroscopic methods. Together with scanning the frequency of the used laser source through the extended minimum of a suitable absorption line filtered Rayleigh and Brillouin scattering (FRS and FBS) are capable of rejecting high levels of stray light from unwanted sources while preserving the spectral information about the physical properties to be measured. When using a laser frequency tuned to the slope of the absorption line the velocity component along the line of sight can be obtained by analyzing the Doppler frequency shift from the scattered Mie signal of particles carried with the flow [4,5,6]. This technique is called filtered Mie scattering (FMS) – also known as Doppler Global or Planar Doppler Velocimetry (DGV or PDV) – and uses the filter principle as a frequency-to-intensity converter.
In this paper we first describe the optical layout of the sensor and then present the various measurement principles regarding the different scatter mechanisms.

2. Sensor Layout

Figure 1 outlines a possible implementation of an optical sensor for temperature, pressure and velocity measurement in a backscatter mode of operation. Laser light is transported via a single-mode polarization maintaining photonic crystal fiber PF (F-SM10-PM from Newport), collimated and focused with lenses L1 (f=10mm) and L2 (f=60mm) into the measurement volume V. A small part of the laser light is guided with a beam splitter BS (splitting ratio 10:90) to a photo diode PD for normalizing the signal with respect to laser power. Due to the use of a single lens for both focusing and collection, light scattered only from this volume can be refocused with L3 (f=160mm) into a second multi-mode receiving fiber RF (multi-mode step index fiber with 100µm core) which transports the collected signal light to the analyzer unit. This confocal arrangement works as a spatial filter to enable measurements in the presence of high background light levels such as in near wall environments. The analyzer unit contains an iodine absorption cell AC and a pair of photomultiplier tubes PM1 and PM2 (Hamamatsu H9305-04 with amplifier C7319). The received light is also split into two parts to allow density normalization in case for Mie signals. The use of an interference filter IF with a FWHM of 1nm (Materion Corp.) blocks all unwanted contributions from broadband background light sources and also most of the Raman components.

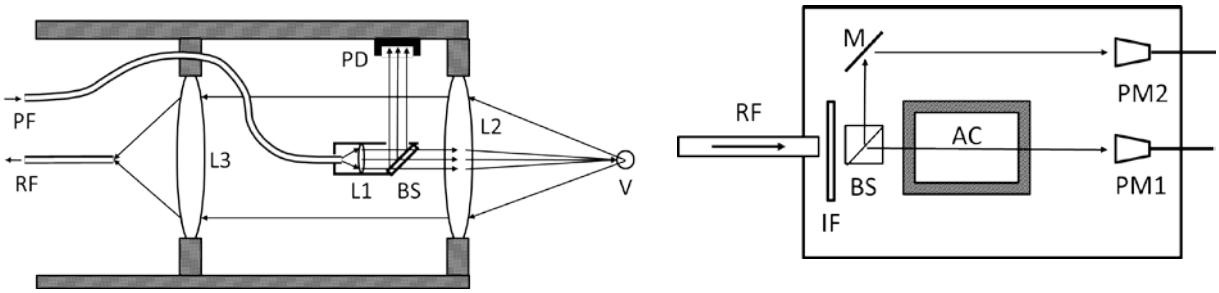

Figure 1 Layout of the optical multi-purpose sensor for collecting backscattered light (left) and the analyzing unit containing the absorption cell (right)

A Verdi-SF-5 (5W, Coherent) DPSS laser system was used as the light source. In combination with a wavemeter (WSU-10 from High Finesse) frequency stabilization and tuning is achieved using two piezos mounted inside the cavity.
Since one objective was the construction of an optical probe with minimal diameter for applications with reduced optical access the final probe design has an outer diameter of 12 mm. Therefore a rather small bore of 12 mm diameter is needed to integrate the sensor into the measurement environment. The length of the sensor head is 200 mm. Traversal of the sensor allows the acquisition of a measurement profile along the sensor axis.
At a laser power of 2W of the transmission efficiency of the photonic crystal fiber (PCF) was approximately 50% such that roughly 1W was available for the probe volume. For a measurement of a data point at a single frequency the acquisition time was set to 2 s. To account for varying signal strength of the different test cases control voltage and gain of the photomultiplier tubes (PMT) were adjusted accordingly.

3. Filtered Rayleigh scattering (FRS)

Elastic scattering from particles (i.e. gas molecules) with diameters much smaller compared to the laser wavelength is called Rayleigh scattering. The spectral profile of such scattered light contains information about physical flow properties like density (via amplitude), pressure (via line shape), temperature (via line width) and even velocity (via frequency shift). It is therefore especially suited to determine multiple flow parameters simultaneously. But in order to do this the spectral information has to be preserved while detecting the signal which can be achieved by using a

suitable spectrometer, sometimes in form of a Fabry-Perot etalon.
The application of this sensor in confined areas often has to deal with strong reflections or stray light from dust and other particles present in the flow which hinders the use of pure Rayleigh scattering as a diagnostic tool. To overcome this problem the Rayleigh scattering technique was expanded by filtering the incoming light with an absorption cell containing a molecular vapor. If the laser frequency is tuned to the center of an absorption line all unwanted light from reflections of dust particles and surfaces can be effectively suppressed. Since the spectral width of the Rayleigh scattered light of a gas is broader than the absorption line width the spectral wings of the Rayleigh part can pass the filter and reach the detector unit (see Figure 2).
An important but seldom appreciated aspect of this method is the conservation of spectral information. The detected signal is a convolution of the Rayleigh spectrum with the spectral filter function. Therefore scanning the laser frequency through regions where the absorption is sufficiently strong to suppress all disturbing Mie signals yields a recorded FRS spectrum which can be used to extract temperature and pressure values by applying a least-square-fit procedure to describe the experimental data with a suitable model (e.g. Tenti S6 [1,5]).
To enhance the resolving power of FRS the spectra in air were recorded at two absorption line centers which happen to exist close together (18788.33 cm^{-1} and 18788.44 cm^{-1}).

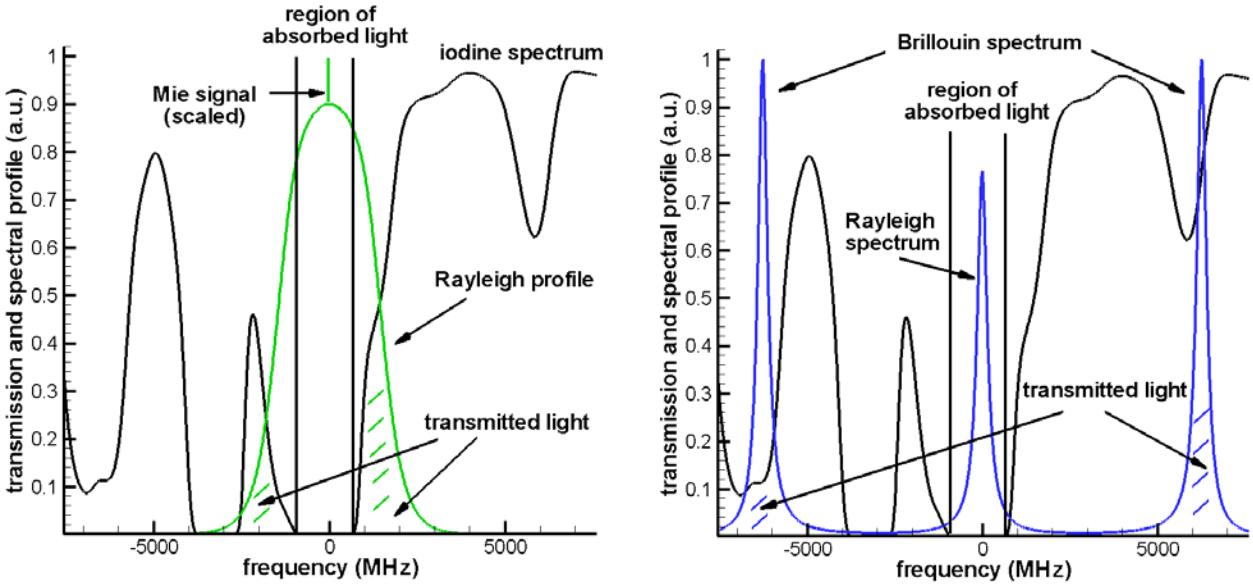

Figure 2 Schematic representation of the measurement principles for filtered Rayleigh scattering (FRS) in a gas (left) and filtered Brilloiun scattering (FBS) in a liquid (right)

3.1 FRS Temperature measurements of gaseous flows

The intensity distribution of the recorded FRS spectrum can be described by a convolution of the Rayleigh spectrum σ_{Ray} with the transmission profile of the corresponding iodine absorption line $t(\nu)$:

$$I_{FRS}(\nu_0) = C_{FRS}\left[\int_{-\infty}^{+\infty} \sigma_{Ray}(\nu - \nu_0, p, T)\cdot t(\nu)d\nu\right] \qquad \text{Eq. 1}$$

The Rayleigh spectrum can be calculated with the help of the so-called S6 model by Tenti and is a function of pressure and temperature. If the medium is moving sufficiently slow the frequency shift of the complete spectrum caused by the Doppler effect can be neglected because these shifts are typically in the order of a few MHz and much smaller than the Rayleigh line width for a gas at

room temperature or higher. For measurements of the bulk flow velocity the use of filtered Mie scattering (FMS) is more accurate and will be discussed in section 5. C_{FRS} contains the geometric efficiency of the experimental set-up and the incoming laser power. Our first application of the sensor was a temperature measurement in a sealed chamber of quartz glass containing air and a heater. To investigate the sensors ability to determine the gas temperature the heating power was varied and the established temperature inside was measured with a commercially available thermo element simultaneously when recording the FRS spectra. The temperature values from the thermo couple were compared with the temperature derived from a least-square-fit applying Eq. 1 to the recorded FRS spectra (Figure 4). As can be seen from Figure 3 the differences between the FRS spectra for different temperatures are very small, especially for temperatures between 23°C and 43°C, as multiple crossings occur.

Only the applied frequency scanning method can distinguish between neighboring profiles and yield a unique solution for a corresponding temperature fit. The pressure inside the glass chamber was also measured with a commercial probe and the value inserted into the fit procedure for temperature. Table 1 shows a good agreement between both measurement techniques, invasive and non-intrusive, which is remarkable if one considers the close proximity of the FRS spectra in this temperature region.

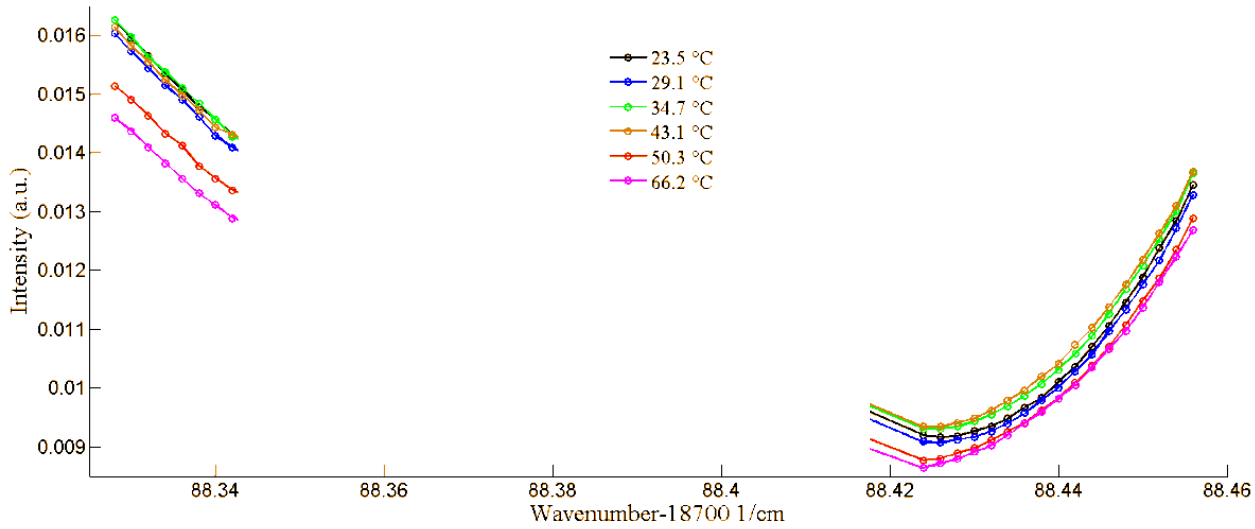

Figure 3 Recorded FRS-spectra in air with different ambient temperatures

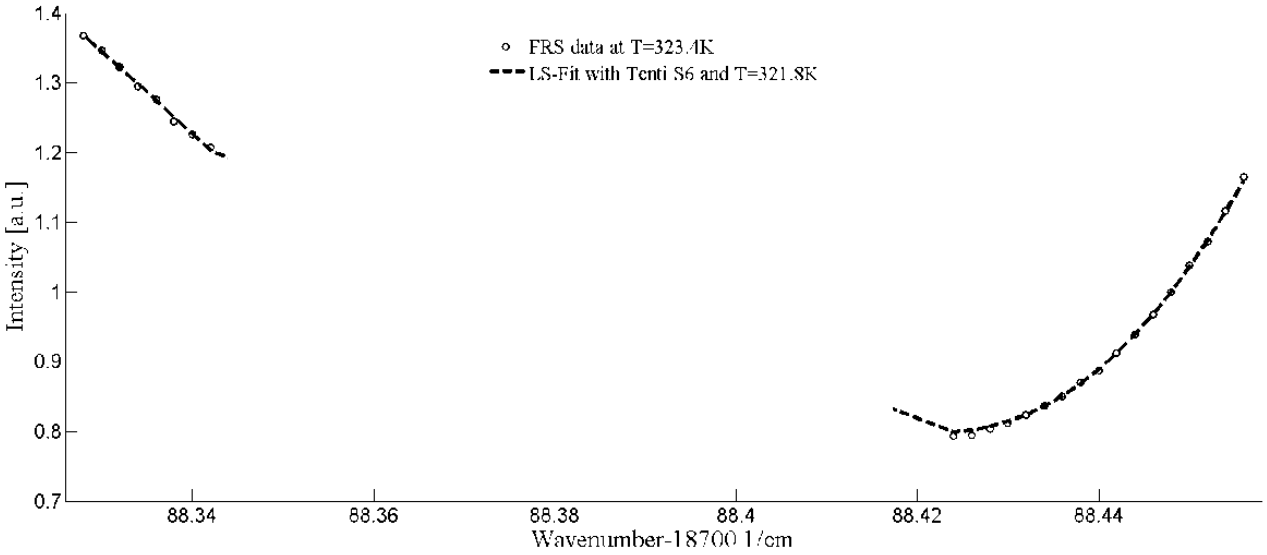

Figure 4 Least-square fit of Eq. 1 to the recorded FRS-spectra in air at 323.4K yielding a temperature of 321.8K

Table 1 Comparison between thermo couple temperature measurements and the values resulting from processing the FRS spectra of Figure 3

T probe [K]	T Fit [K]	Delta [K]	Delta [%]
296,6	296,8	0,15	0,1
302,3	298,6	-3,65	-1,2
307,9	309,7	1,85	0,6
316,3	319,7	3,45	1,1
323,4	321,8	-1,65	-0,5
339,4	343,6	4,25	1,3

3.2 FRS Pressure measurements of gaseous flows

The determination of pressure in a gas is analogous to the procedure for temperature measurements as described before. A small chamber which could be pressurized up to 10bar was used for recording FRS spectra in air at varying pressures. The temperature inside was measured with the thermo couple and a pressure probe was used to determine the reference values for comparison with the sensor data. All the data points of a recorded FRS spectrum are fitted with Eq.1 containing this time the pressure value as the unknown quantity. Figure 5 shows the evolving shapes of the FRS spectra with increasing pressure from 1 bar to 8 bar. In contrast to the temperature spectra the pressure spectra don't show any crossings and vary in intensity and shape uniquely with increasing pressure values.

As can be seen from the deviations of the least-square fit results from the pressure values measured with the commercial probe in table 2 the agreement of the FRS measurements with these values is getting worse with increasing pressure. The reason seems to be a problem of the model function for higher pressures because figure 6 shows systematic deviations between the data points and the theory. Further investigations are required to examine this feature. Reducing this discrepancy will

directly lead to a better measurement accuracy.

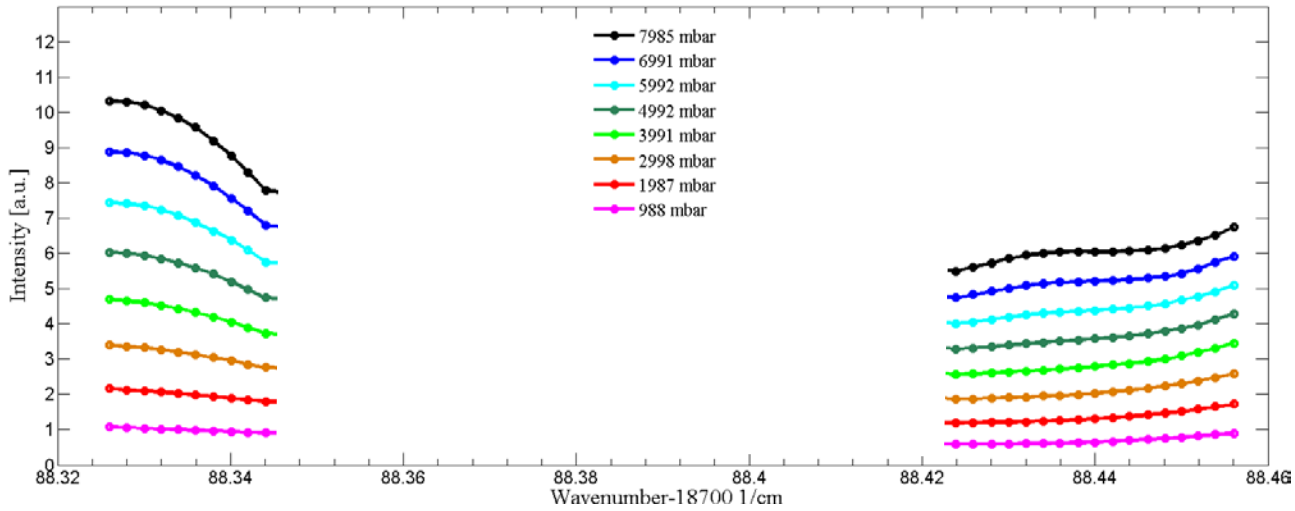

Figure 5 Recorded FRS-spectra in air with different chamber pressures

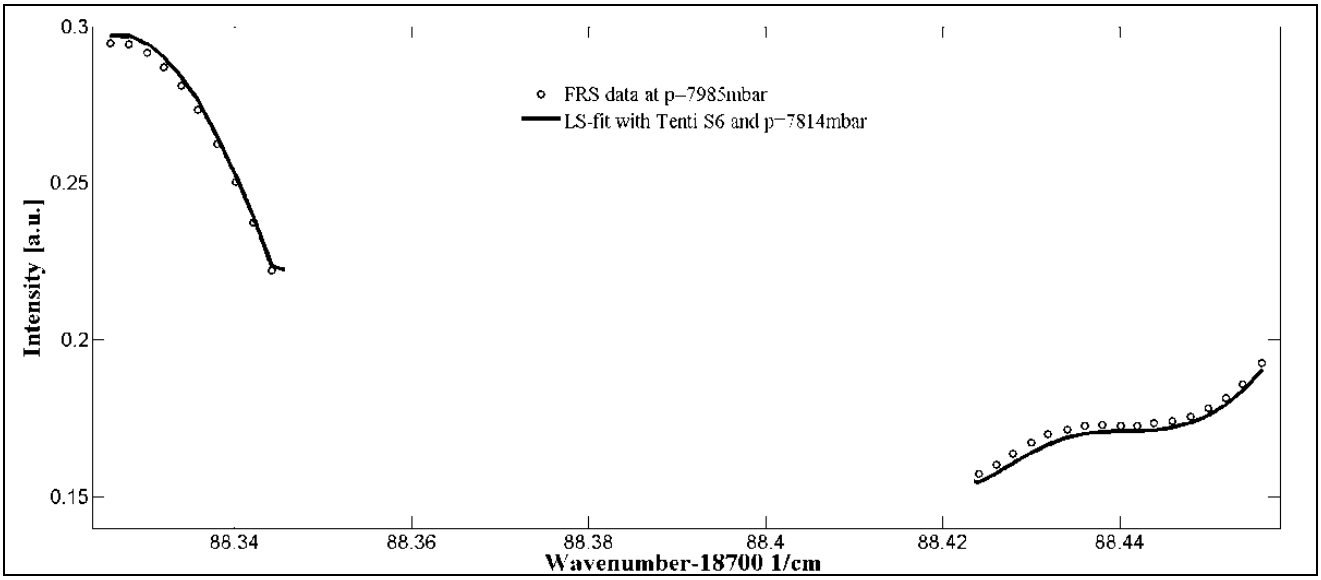

Figure 6 Least-squares fit of Eq. 1 to the recorded FRS-spectra in air at 7986 mbar yielding a pressure of 7814 mbar

Table 2 Comparison between probe pressure measurements and the values resulting from processing the FRS spectra of Figure 5

P probe [mbar]	P fit [mbar]	Delta [mbar]	Delta [%]
1987	1970	-17	-0,9
2998	2951	-47	-1,6
3991	3920	-71	-1,8
4992	4891	-101	-2
5992	5868	-124	-2,1
6991	6844	-147	-2,1
7985	7814	-171	-2,1

4. Filtered Brillouin scattering (FBS)

The spectrum of light scattered from liquids like water consists of two pronounced Brillouin peaks separated from a weaker Rayleigh signal (Figure 2, right). The latter signal together with the contribution of suspended particles in the fluid is effectively blocked analogous to the Mie signals in case of FRS. Furthermore the typical Raman signal which is shifted around 100nm from the laser line is easily blocked by the interference filter in the analyzer unit. In contrast to FRS in a gas the Brillouin peaks for water are separated by 6-7 GHz from the laser frequency and the sensitivity to a temperature change of the liquid is dependent on the iodine absorption spectrum at these positions and not the central absorption line shape. Figure 7 and Figure 8 illustrate this fact: While laser frequencies around 18788.33 cm^{-1} and 18788.44 cm^{-1} produce Brillouin peaks at places where the iodine spectrum has no sharp absorption features, that is, small absorption gradients, laser frequencies around 18789.28 cm^{-1} produce peaks that correspond to another two absorption centers of iodine. While this is coincidental it has the advantage of providing a high sensitivity for FBS spectra with changing temperature as can be seen from the scan shown in figure 9.

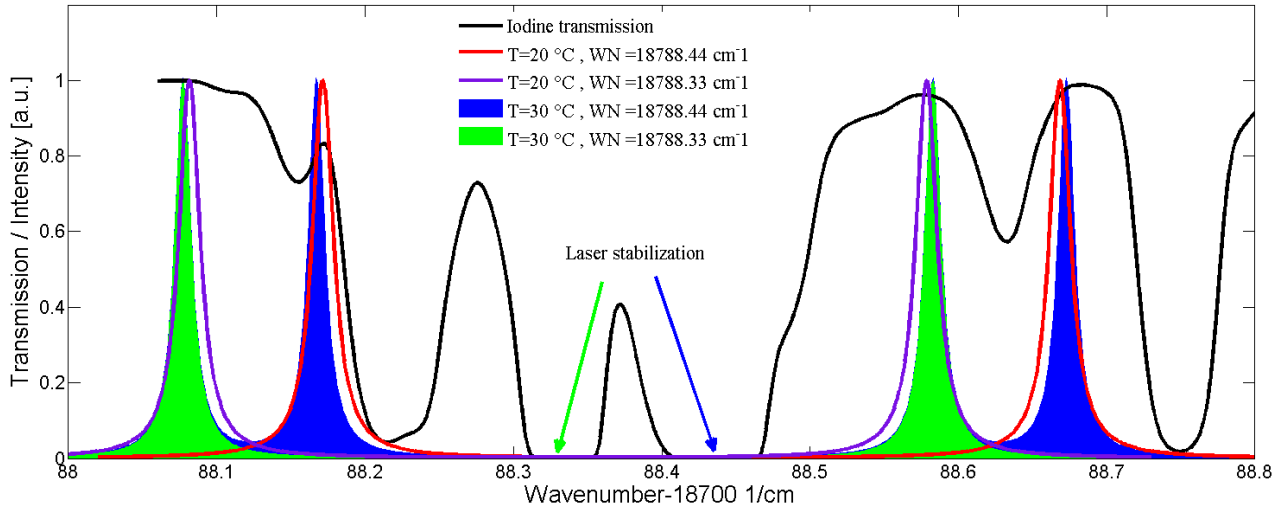

Figure 7 Two Configurations (18788.33 cm^{-1} and 18788.44 cm^{-1}) for FBS in water with a low sensitivity for temperature change

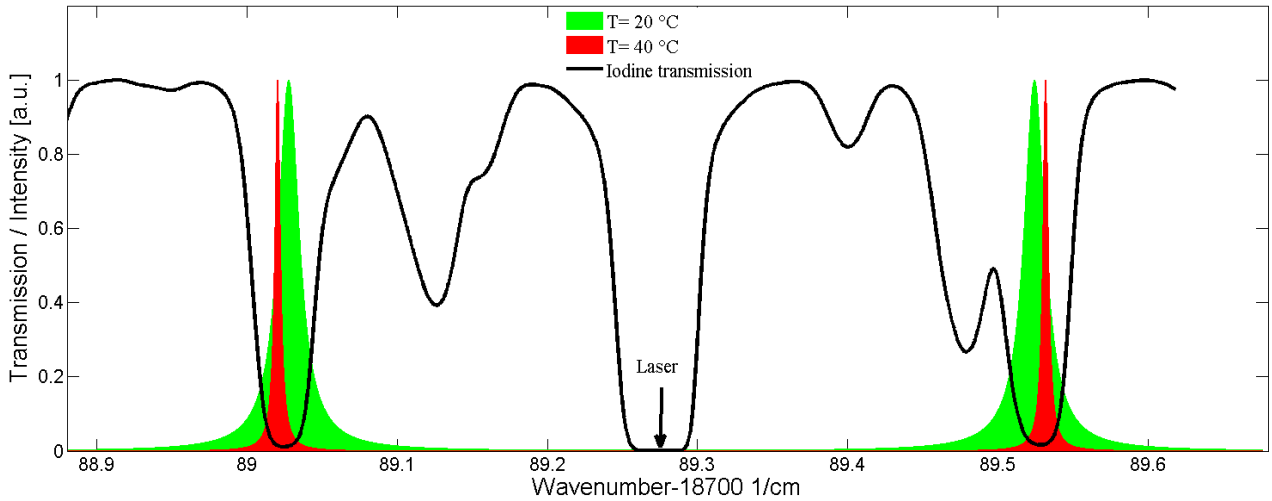

Figure 8 Configuration (18789.28 cm^{-1}) for FBS in water with a high sensitivity for temperature change

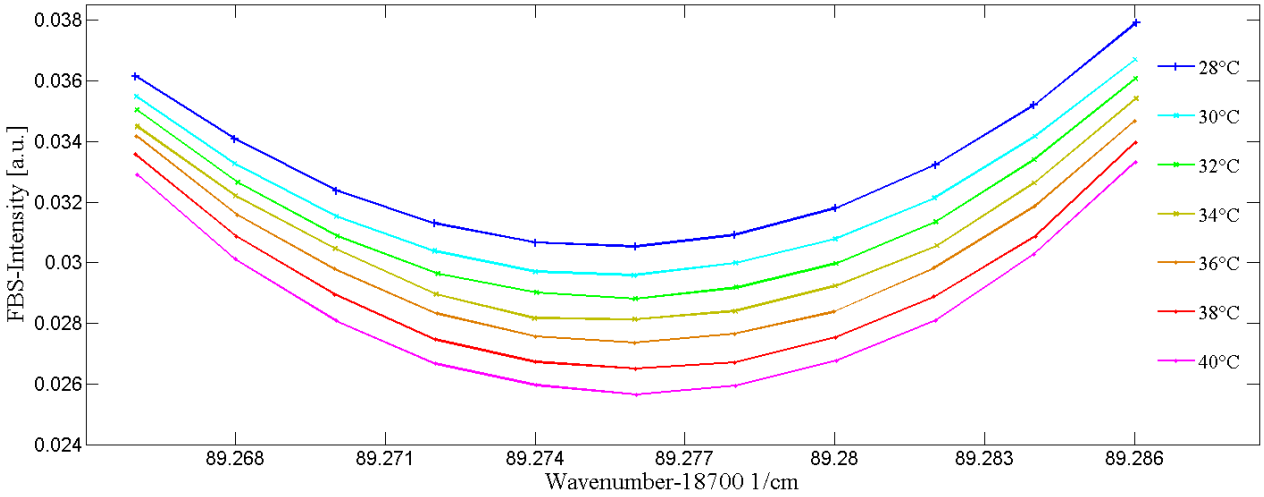

Figure 9 FBS temperature scans in tap water

4.1 FBS Temperature measurements of liquids

The frequency shift $\Delta\nu_s$ of both Brillouin peaks relative to the laser frequency is dependent on the velocity of sound c_s and the refraction index n which are both well-known functions of temperature as given in:

$$\Delta\nu_B = \pm\frac{2c_S(T)n(T,\lambda)}{\lambda} \qquad \text{Eq. 2}$$

Therefore the spectrally resolved FBS signal which is a convolution of the Brillouin spectrum S(v) with the iodine absorption spectrum can be used to determine the temperature of the liquid using Eq 3 together with the iodine transmission curve for a description of the filtered Brillouin spectrum:

$$S_B(\nu,\Delta\nu_B,\delta\nu_B) = \frac{I_B}{2\pi}\left(\frac{\delta\nu_B/2}{(\nu-\Delta\nu_B)^2+\left(\delta\nu_B/2\right)^2}+\frac{\delta\nu_B/2}{(\nu+\Delta\nu_B)^2+\left(\delta\nu_B/2\right)^2}\right) \qquad \text{Eq. 3}$$

At the same time the line width $\delta\nu_B$ of these peaks also are functions of temperature which to date has received little attention in the literature. In order to improve the fit function Eq 3 was fitted to the recorded FBS spectra in dependence of the temperature parameter in order to calibrate the line width. An example of the fit quality is shown in Figure 10.
The final result is presented in Figure 11 which compares the determined line widths to the literature data of Fry et al [2]. Using this function for the Brillouin line widths a measurement of water temperatures with accuracy in the order of 0.1K seems feasible.

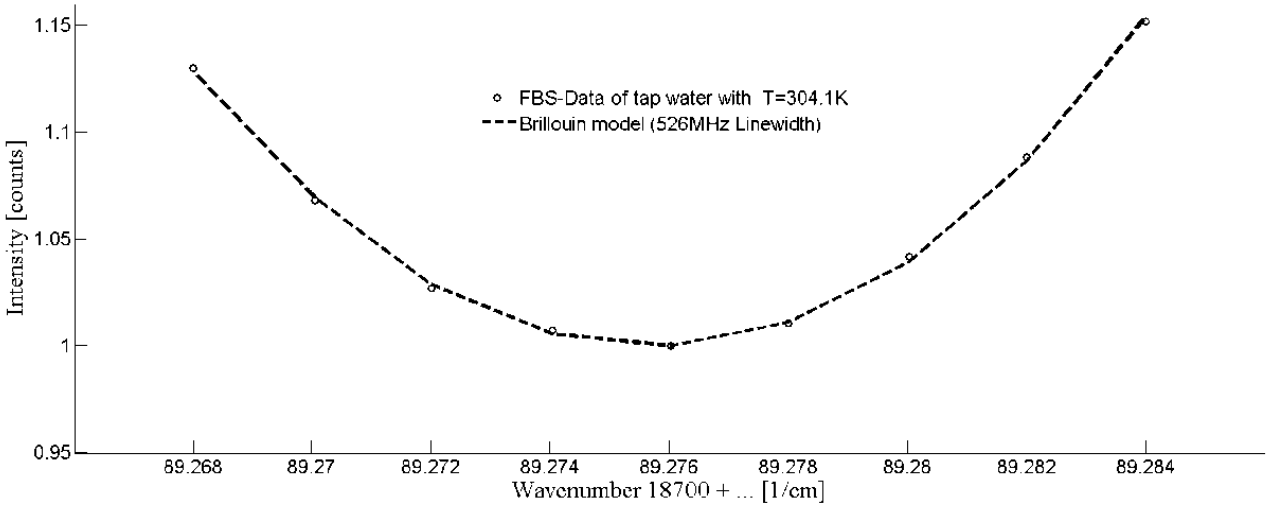

Figure 10 Least-squares-fit of Eq 3 to the FBS data with T=304.1K yielding a line width of 526 MHz

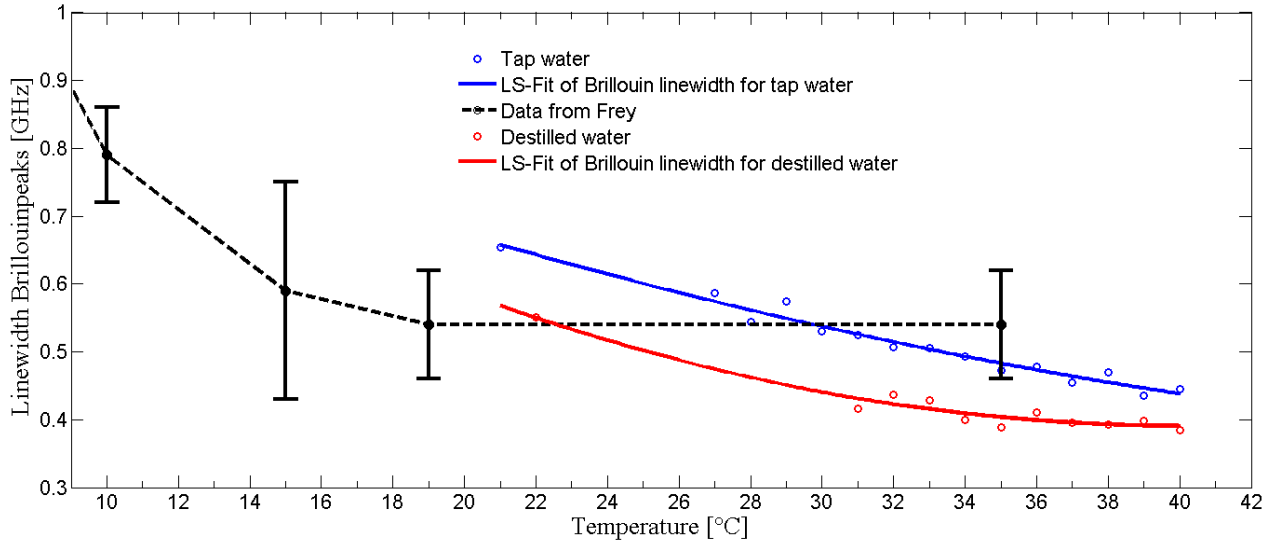

Figure 11 Comparison of determined Brillouin line widths of water with experimental data from Fry [2]

5. Filtered Mie scattering (FMS)

Velocity measurements are possible by exploiting the Doppler Effect which produces a frequency shift of the scattered light relative to the incoming light frequency if the scattering particles are moving with the flow. Although Rayleigh and Brillouin spectra are also shifted by this effect the possible frequency resolution with FRS and FBS is not sufficient due to their broad spectral width especially for resolving small shifts in the order of a few MHz. But in the presence of suitable particles in the flow (i.e. seeding particles) the resulting Mie signal can be used to determine the Doppler frequency shift with sufficient accuracy when using the slopes of an absorption line. The iodine cell converts the frequency change into a transmission change which has the highest sensitivity at the slopes. Scanning the laser frequency over a complete absorption line and determining the frequency shift with a least-square-fit of an unshifted line profile yields the most accurate measurement of one velocity component.

5.1 FMS Velocity measurements of seeded flows

Using a pure backscatter arrangement the sensor determines the line-of-sight component of the

flow velocity V_{LOS} from a measured frequency shift Δν via the relation:

$$\Delta\nu = \frac{2\nu_0}{c} V_{LOS} \,. \qquad \text{Eq. 4}$$

Figure 12 shows several shifted absorption profiles corresponding to different flow velocities of a simple free-jet experiment in air with small paraffin oil droplets added as scatter particles to the flow. The core velocity of the jet was calculated using isentropic relations and probe measurements of pressure and temperature values inside a settling chamber. The sensor axis was aligned in a 135° backscatter configuration relative to the flow direction of the free jet.
The reference transmission curve was recorded with a glass vessel in front of the sensor filled with paraffin oil droplets added to the air fluid in rest. Applying a least-square-fit procedure the frequency shift was determined comparing the shifted transmission profile for a given velocity to the spectrum for the fluid in rest (see fig. 13). Table 3 exhibits a good agreement between the jet core velocities and the values measured by the sensor.

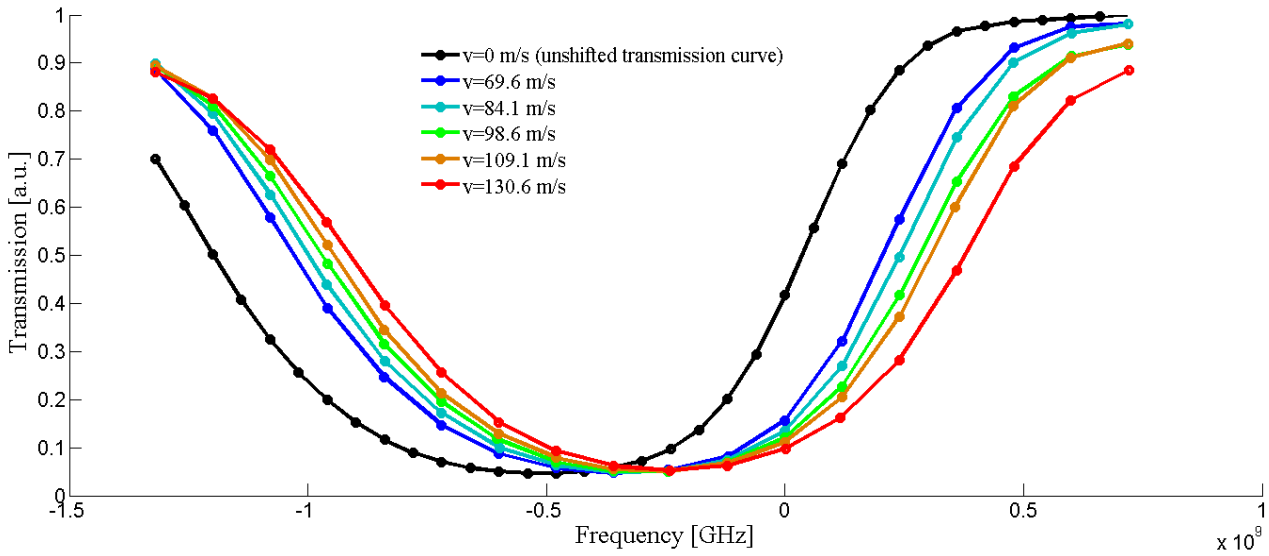

Figure 12 FMS velocity scans of a free-jet experiment

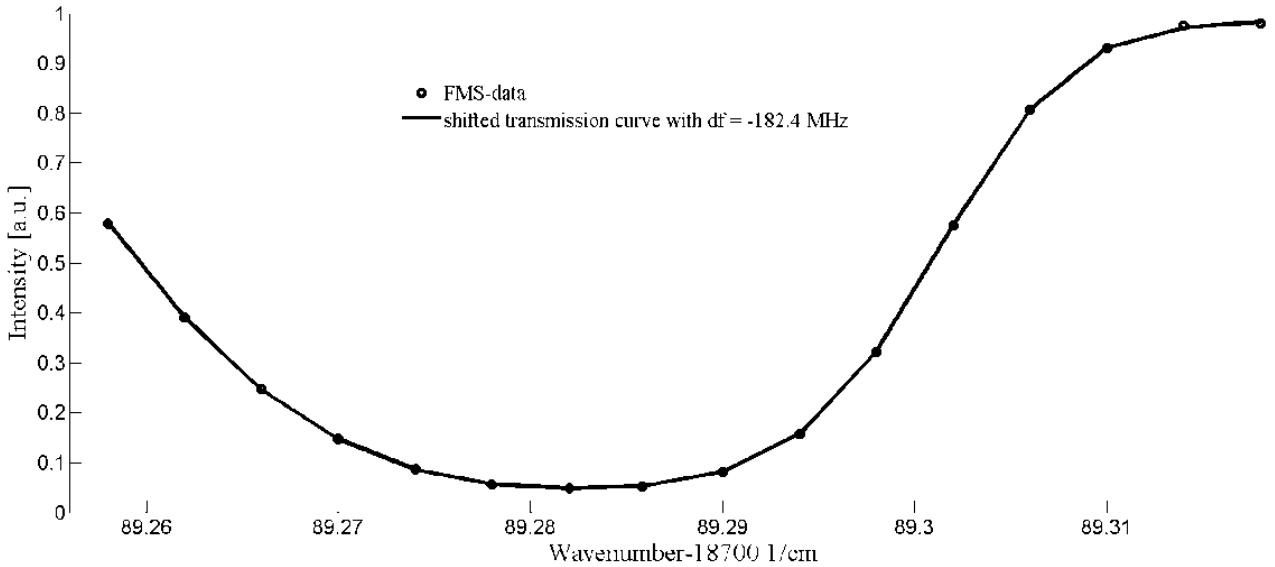

Figure 13 Least-square-fit of a shifted absorption line to the unshifted transmission curve yielding a frequency shift of -

182.4 MHz

Table 3 Comparison between jet velocities determined with isentropic relations and the values resulting from processing the FMS spectra of Figure 12

V jet [m/s]	V Fit [m/s)	Delta [m/s]	df jet [MHz]	df Fit [MHz]	Delta [MHz]	Delta [%]
69,64	68,63	-1,01	-185,12	-182,44	2,68	1,5
84,08	81,82	-2,26	-223,51	-217,51	6	2,7
98,55	99,03	0,48	-261,98	-263,24	-1,26	0,5
109,01	107,7	-1,31	-289,78	-286,29	3,49	1,2
130,99	130,62	-0,37	-348,21	-347,23	0,98	0,3

6. Conclusions

In this paper we presented an optical sensor capable of measuring temperature, pressure and velocity in different media. The layout of the probe head in backscatter configuration allows production and detection of scattered light signals from a single optical access port. Minimization of the sensor diameter was given a high priority to allow applications in confined environments with limited access. The sensor is currently optimized for stationary measurements given the fact that the measurement principle rely on frequency scanning methods.

One limitation of the current probe design is the difficult alignment of the receiving fiber inside the 12 mm tube which reduces the collection efficiency to 20% of the estimated theoretical value. An increased inner diameter will lead to a significantly better alignment of the receiving fiber inside the sensor.

As simple proof-of-concept experiments the scattered signals in air with and without seeding particles and water at room temperature were recorded and processed. Table 4 summarizes the performance of the sensor with respect to the different measurement techniques. While the intensity of FBS and FMS signals are two orders of magnitude higher than the FRS signals the spectral form of the profiles also differ from each other due to their different overlap with absorption regions of the iodine spectrum while scanning the laser frequency.

We intend to further develop the sensor with respect to possible acquisition times, spatial resolution and accuracy for multiple applications like near-wall measurements and confined duct experiments.

Table 4 Summary of the sensor performance with respect to different measurement applications

Tech.	Parameter	Medium	P(bar)	T(K)	V(m/s)	Rel.Acc.(%)	Intensity (a.u.)
FRS	T	air	1	300-350	0	1-2	0.01
FRS	p	air	1-10	300	0	2	0.01 - 0.1
FBS	T	water	1	300-350	0	<0.3	1
FMS	v	air+seeding.	1	300	0-100	1-2	10

List of References

[1] Doll U, Fischer M, Stockhausen G, Willert C (2012) Frequency scanning filtered Rayleigh scattering in combustion experiments. Intern Symp on Applications of Laser Techniques to Fluid Mechanics Lisbon, Portugal, 09-12 July, 2012

[2] Fry E, Katz J, Liu D, Walther T (2202) Temperature dependence of the Brillouin linewidth in water. J Modern Optics **49**(3-4):411-418

[3] Hair J W, Caldwell L M, Krueger D A, She C Y (2001) High-spectral-resolution LIDAR with iodine-vapor filters: measurement of atmospheric-state and aerosol profiles. Appl Opt **40**(30): 5280-5294

[4] Meyers J F, Lee J W, Schwartz R J (2001) Characterization of measurement error sources in Doppler global velocimetry. Meas Sci Technol **12**:357-368

[5] Miles R B, Lempert W R, Forkey J N (2001) Laser Rayleigh scattering. Meas Sci Technol **12**: R33–R51

[6] Roehle I, Schodl R, P Voigt, Willert C (2000) Recent developments and applications of quantitative light sheet measuring techniques in turbomachinery components. Meas Sci Technol **11**:1023-1035

[7] Schorstein K, Popescu A, Goebel M, Walther T (2008) Remote water temperature measurements based on Brillouin scattering with a frequency doubled pulsed Yb:doped fiber amplifier. Sensors **8**:5820-5831